Using ABAQUS to Understand Media Transport

Ted Diehl[1]
Manager: CAE Systems, GP&IM
Xerox Corporation
Webster, New York

ABAQUS User's Conference Proceedings
Newport, Rhode Island
May 29 - 31, 1996

Abstract

Analyzing the transport of flexible sheet media such as paper or film has traditionally been difficult due to the complexities of large displacements and rotations, buckling, nonlinear material behavior, moving boundary conditions, and intermittent contact with friction. This paper reviews techniques of analyzing media transport issues with the nonlinear finite element methods available in ABAQUS. We will show how a large variety of ABAQUS options, ranging from 2-D structural elements to 3-D continuum elements, linear material representations to complex hyperelastic material laws, implicit quasi-static and dynamic techniques to explicit dynamic approaches, and several specialized user subroutines, can be used to study this class of problems.

1.0 Introduction

The effectiveness of today's office environment relies heavily on the use of copiers, printers, and facsimile machines. Undesirable equipment behavior, such as sheet jams, image skew, misregistration, and image artifacts like smearing or ghosting can all be caused by improper media handling. Because of this, media transport technology is vital to these systems and can affect almost everyone on a daily basis.

Figure 1 depicts a few fundamental issues that an engineer must consider when designing media transport systems. Figure 1a depicts a common tire-based nip system used in copiers. Engineers must understand how an elastomeric roller will interact with a sheet of paper or transparency. Variables that must be evaluated include elastomer material characteristics, roller geometry, deformation, and friction (as well as variations in these parameters). Simple calculations used to assess these variables are frequently not adequate, leaving design engineers puzzled as they try to explain their unexpected test results. Figure 1b depicts another common scenario that must be understood. How will the sheet transport in a confined space? Will it buckle severely and jam?

1. Based on previous work performed by the author at Eastman Kodak Company and on the Ph.D. dissertation of Diehl (1995b) at the University of Rochester.

Analyzing this type of problem with traditional linear beam analysis will usually not suffice due to the large deflections and varied, initially unknown, contact conditions.

Because media transport problems are complex and exhibit many severe nonlinearities, it is frequently necessary to make simplifying assumptions. We usually decide to focus on one of two main areas: 1) concentrate on the deformations of the flexible media and utilize simplified boundary conditions to approximate the effects of the rollers, or 2) concentrate on the deformations of the rollers and utilize simplified representations of the media. Although fully coupled models are sometimes possible, any increase is simulation accuracy does not typically justify the significant increase in computational effort.

Several *individual* solutions to many of these problems have been presented in the past literature. For brevity, we will only mention a few citations. The book by K. L. Johnson (1989) and papers by Soong and Li (1980, 1981a,b) provide excellent overviews of many linear elastic, small deformation nip studies.[1] For problems of the type shown in Figure 1b, finite difference programs based on equations of the Elastica have been traditionally used.[2]

Unfortunately, engineers tasked with understanding a variety of these media transport issues typically do not leverage previous work in the literature. The most common reasons stated are: 1) it takes too long to search-out and understand a published study and 2) many of the solutions utilize complex, specially-made numerical algorithms that are non-trivial to code. On the other hand, if a single commercial software package could be used for such analyses, then it is likely that more engineers would leverage it. This paper will review several previous works by the author to demonstrate that many media transport issues can be successfully studied using ABAQUS.

2.0 Flexible Sheet Transport Models

In this section, we show how ABAQUS/Standard is utilized to perform quasi-static and inertial dynamic simulations of media transport. The models in this section concentrate on the flexible media and utilize simplified boundary conditions to simulate the roller influence on the media. Three example problems (Figures 2 - 4) from Diehl (1993a,b) highlight several capabilities of ABAQUS/Standard for this class of analyses. Figures 2 and 3 are quasi-static solutions with the following parameters: elastic modulus of 1.64×10^9 Pa, shear modulus of 8.21×10^8 Pa, and mass density of 740 kg/m^3. The dynamic simulations of Figure 4 use an elastic modulus of 1.29×10^9 Pa, shear modulus of 6.45×10^8 Pa, and mass density of 684 kg/m^3. The sheet in all solutions has a width (Z direction) of 279 mm, a thickness of 0.102 mm, and is modeled with hybrid beam elements to improve convergence speed. For simplicity, all three examples ignore friction[3], electrostatic, and aerodynamic effects. Since only elastic deformations of the sheets are considered,

1. Further background on linear and nonlinear nip mechanics as well as hyperelastic material modeling for both incompressible and foamed elastomers can be found in Diehl (1995b,c) and Stack (1995).

2. See Timoshenko (1961), Benson (1981), or Stack et al (1994) for details on the theory of the Elastica.

3. See Diehl (1995a) for methods to improve ABAQUS/Standard predictions when using friction.

the *BEAM GENERAL SECTION option is used instead of the *BEAM SECTION option for defining the beam element properties of the sheet. This can save in some cases up to 35% CPU time since numerical integration through the thickness of the beam is avoided at each iteration.

The example in Figure 2 depicts how the drive nip's influence on the sheet is simulated. As it moves through the nip, the sheet is clamped by the rollers and subjected to an enforced displacement in the X direction. The boundary conditions for the sheet under the nip are

$$u_x = \text{specified} \qquad u_y = 0 \qquad \theta_z = 0 \tag{1}$$

This is simulated with a user-supplied MPC (Multi-Point Constraint) subroutine (Diehl, 1993a,b). As nodes on the sheet pass the drive nip location, the MPC constraint is removed. This user subroutine approach is very efficient and easy to use for many industrial-class problems.

Also depicted in Figure 2 is the calculation of relative velocities for the tip of the sheet as it moves on a circular drum. The relative velocities, ignoring inertial dynamic effects, are computed from the quasi-static solution using three-point Lagrange polynomial finite difference derivatives (see Diehl 1993b and Burden 1985). Since the time scale is purely artificial, only relative velocities between two different nodes are meaningful.

The example in Figure 3 demonstrates how initial sheet curl is simulated. Diehl (1993b) has shown that initially curled media can be modeled by enforcing an initial stress state (via moments) into a flat (straight) sheet. Based on beam-bending equations, curl defined by an initial radius of curvature R is related to the initial bending moment M by

$$M = \frac{EI}{R} \tag{2}$$

where E is the elastic modulus and I is the area cross-sectional moment of inertia for the beam. Equation 2 is valid for large rotations and small strains. In ABAQUS/Standrd, this initial moment is applied using the *INITIAL CONDITIONS, TYPE=STRESS option.[1] This approach keeps the input deck simple and makes the solution very efficient. Using a *non-flat initial geometry* (curled) makes the deck significantly more complex because of the additional steps required to feed the sheet through the drive nips.

Curl can also be introduced by applying a thermal strain gradient across the thickness of the media. From beam theory, it is easy to show that an applied temperature gradient, T', through the thickness of the sheet is related to the radius of curvature (curl) as

$$T' = \frac{-1}{\alpha R} \tag{3}$$

where α is the coefficient of thermal expansion. If we choose α to be unity, then the radius of curvature is inversely proportional to the applied temperature gradient in the sheet. This method

1. If using *BEAM GENERAL SECTION, the values input for *IINITIAL CONDITIONS are initial section forces and moments, not initial stresses.

also yields a simplified deck as before (initial geometry of sheet defined straight) but has the added benefit of being able to modify the amount of curl at any time during the analysis.[1] This allows for the simulation of process induced curl. Furthermore, this approach is easily extended to shell models.

All the solutions from Figure 2 - 4 correlate well with the benchmarks provided. Also important to note is that the calculations for these problems were fast. The solutions, computed on a Sun SPARCstation 10-30, ranged from 82 CPU seconds to 295 CPU seconds.

3.0 Sheet Registration and Alignment Models

Understanding sheet registration and alignment has become increasingly important to customers as we head into the digital age. Figures 5 and 6 demonstrate how both nonlinear beam and shell models are utilized to study a buckle registration system. A complete alignment model would require feeding a sheet, represented with nonlinear shell elements, through a complex channel. In general, this type of model is prohibitively expensive and difficult to compute. Instead, we simplify the study into two analyses: 1) analyze the sheet transport with a beam model, and 2) analyze the sheet alignment with a shell model.

The ABAQUS/Standard quasi-static beam transport model shown in Figure 5 evaluates sheet accumulation during buckle, feed loads required to produce the buckle, and the shape of the sheet inside the channel. The contact conditions between the sheet and channel change significantly throughout the analysis. In general, the channel is defined as a master surface and the nodes on the sheet are defined as slave nodes. This is true for all contact except where the channel has sharp edges. At these locations, the definition of slave and master is switched. Dummy nodes are defined on and constrained to the channel at these locations. A separate contact pair definition is defined so that these dummy nodes become slaves and the surface of the deformable sheet is the master. Using this technique improves convergence speed and significantly reduces solution chatter caused by ratcheting from the discretized contact.[2] This solution also uses the SOFTENED contact option to improve convergence speed and solution robustness.

The sheet deformation in Figure 5c is highly buckled. Future research will look at computing even "higher modes" of post buckled deformations. Models such as those depicted in Figure 5c have difficulty predicting further buckling because the sheet needs to snap (unstably) from one side of the channel to the other. Current quasi-static solution attempts, even with a Riks algorithm, will not work. Future studies will likely look at the use of viscous contact or "slow dynamics." However, these investigations must be done with caution because such numerical tricks may improperly influence the results due to the sheet being transported.

---

1. The temperature gradient is an applied load defined in the step section of the deck.

2. See Diehl (1995a) for a general discussion about switching definitions of master and slave for sliding contact.

Figure 6 demonstrates how a quasi-static nonlinear shell model can be used to assess sheet alignment. In the actual physical problem, the lead edge of a sheet attempts to align with a registration gate which may be rotated by some small amount (about the y-axis) relative the lead edge of the sheet prior to initial contact. As a corner of the sheet hits the gate, the sheet begins to buckle (storing energy). The portion of the sheet's lead edge that is not in contact with the gate will potentially align to the gate due to the release of the stored energy in the buckled sheet. A complete analysis of this process is quite expensive because of contact, buckling, stability, and shell issues. Thus, we simplify the analysis to study the fundamental mechanism.

Figure 6a demonstrates how the analysis is performed. A BEAM MPC that pivots about one corner of the sheet's lead edge is utilized to simulate the gate. The sheet is first buckled to a given height while the lead edge is kept parallel with the trail edge. Then the lead edge is rotated about the y-axis. By evaluating the reaction moment from the MPC's independent node at the pivot point, we can determine if the sheet is pushing against the gate (MPC). As long as the moment is negative, the sheet would remain in contact with the gate. Once the moment becomes positive, then the gate would have to pull on the sheet to keep contact (not physical). Hence, maximum alignment is found when the moment equals zero.

From Figure 6e we find three solutions with zero moment. Which solution should the engineers use to guide their design? The answer lies in an evaluation of solution stability and internal strain energy. The tangent stiffness of the moment-rotation plot in Figure 6e is defined as

$$K^t = \frac{dM_y}{d\theta_y}, \qquad \begin{array}{ll} K^t > 0 & \rightarrow \text{ stable} \\ K^t < 0 & \rightarrow \text{ unstable} \end{array} \tag{4}$$

As long as K^t is positive, the solution is stable and physically possible. When K^t is negative, the solution is unstable and not physically possible.[1] This assessment narrows down the possible physical solutions to b or d.

For a conservative prediction, we should select point b. However, we can utilize the plot of stored internal energy (Figure 6f) to determine if the less conservative prediction of d is likely. To move from point b to point d, we must be able to overcome the energy barrier that peeks at location c. Since the solution we computed is only static, no consideration has been given to dynamic effects. A calculation of the kinetic energy in the sheet, based on its mass and actual speed, can be used to determine if there is enough energy in the system to overcome the energy barrier. If this amount is greater than the energy barrier, then the less conservative prediction, d, may be the best one.

1. The sheet would not stay in that configuration, but rather change shape to some other *stable* configuration.

4.0 Nip Mechanics Models

The models in this section concentrate on the deformations of the elastomeric rollers while utilizing simplified representations of the media. Solutions presented summarize the work of Diehl (1995b,c). The analyses address the study of elastomeric tires, ranging from solid rubber to foam, transporting sheets under large strain conditions (> 15% compressive nominal strain). For certain problems, deformations that exceed 50% compressive nominal strain are presented. These analyses utilize continuum elements (both 2-D and 3-D), hyperelastic material representations, and both implicit and explicit solution approaches.

Traditionally, rollers have been made out of solid rubbers. Recently, designers have investigated foams and foamed rubbers. To cover this range, Diehl studied three actual materials, solid urethane and two foamed elastomers.[1] The first foamed material, R600U, is a highly compressible polyester-based open-cell polyurethane foam with an average density of 80 kg/m^3 in the undeformed state. The second foamed material, SE410, is a moderately compressible closed-cell EPDM (ethylene propylene diene methylene) expanded rubber with an average density of 160 kg/m^3 in the undeformed state. All material models here assume purely elastic response. For solid rubbers, such as urethane, Hooke's law or a neo-Hookean model can be used because urethane's material response is relatively linear up to near 50% deformation (a value far exceeding typical copier applications). For the foamed rollers, nonlinear effects occur at much lower strains (say 10%). Furthermore, foamed rollers are typically deformed to greater strains than solid rubber rollers. For brevity, we will only concentrate on foamed roller modeling here.

The strain-energy function used to model the foams is an Ogden-Hill formulation (*HYPERFOAM material representation in ABAQUS). The Ogden-Hill strain-energy density function per unit original volume is

$$W = \sum_{n=1}^{N} \frac{2\mu_n}{\alpha_n^2}\left[\left(\lambda_1^{\alpha_n} + \lambda_2^{\alpha_n} + \lambda_3^{\alpha_n} - 3\right) + \frac{1}{\beta_n}\left(J^{-\alpha_n\beta_n} - 1\right)\right] \tag{5}$$

where μ_n, α_n, and β_n represent material parameters, N is the number of finite terms in the series, and the principal stretch ratios and elastic volume ratio are defined by λ_i and J, respectively. The initial tangent shear modulus based on Hooke's law, μ_0, as computed from a simple-shear deformation mode (Figure 7), is

$$\mu_0 = \sum_{n=1}^{N} \mu_n . \tag{6}$$

The material parameters, β_n, are related to the generalized Poisson's ratios, ν_n, by

1. The foamed elastomers were supplied by Illbruck, Incorporated. See Diehl (1995b) for a more detailed treatment of the material behavior of all three materials. Also see Stack (1995) for additional studies of elastomeric rollers.

$$\beta_n = \frac{\nu_n}{1 - 2\nu_n}. \tag{7}$$

To obtain the appropriate constants (μ_n, α_n, β_n, and N) for a given material in question, physical testing is required. Figure 7 depicts the deformation modes tested and Figures 8 and 9 present the reduced material data and resulting Ogden-Hill material representations. As seen in both figures, the model represents the data well. Two other material laws for foamed rubber, the Blatz-Ko (1962) model for polyurethane foam and the Brockman (1986) model for moderately compressible material, were also evaluated by Diehl (1995b).[1] Neither of these laws could satisfactorily represent the material behavior for these particular materials beyond 5% strain. Diehl (1995b) also did a thorough assessment of Drucker Stability to make sure that the material parameters listed in Figures 8 and 9 are valid.

Figure 10 presents evaluation of a SE410 tire compression test. Deformations range up to 60% nominal effective radial strain, where

$$\varepsilon^{\text{eff}} = \frac{B_o - B}{B_o} \tag{8}$$

Correlation between the FE model and experiments is excellent. The solution is computed with ABAQUS/Standard. Similar results are found using ABAQUS/Explicit.

Figures 11 and 12 summarize results for predicting sheet motion. Inertial dynamic effects are not of interest. Only quasi-static predictions are desired. Quasi-static solutions using ABAQUS/Standard, an implicit method, were not robust because of convergence difficulties caused by the ever-changing frictional contact.[2] As a result, the solutions were computed with ABAQUS/Explicit. The Explicit approach yielded more robust solutions. However, this method required extra effort to minimize the dynamic ringing and other artifacts commonly found with explicit dynamic calculations (See Diehl, 1995b, for more details).

For elastomeric nip systems, sheets travel at speeds that are different than those predicted by a simple tangential-speed calculation using the undeformed (or deformed) roller radius. The ratio of the actual transport speed, v, to the nominal (undeformed) calculated speed, v_0, is termed the *speed ratio*, denoted as $\tilde{v}$. If the speed ratio is greater than one, the sheet is said to *overdrive* the feed rollers. When the speed ratio is less than one, the sheet is said to *underdrive* the feed rollers. Whether the sheet overdrives or underdrives the feed rollers is strongly dependent on the mechanical properties of the elastomers and the amount of external load applied to the nip system.

---

1. Both of these laws are subsets of the general Ogden-Hill form. Blatz-Ko is found by setting $N = 1$, $\alpha_1 = -2$, $\beta_1 = 1/2$, and $\mu_1 = \mu$. Brockman is found by setting $N = 1$, $\alpha_1 = 2$, $\beta_1 = \nu / (1 - \nu)$, and $\mu_1 = \mu$.

2. Stack (1995) has developed a more robust implicit finite element solution that is capable of modeling rolling contact. His solutions do not display such convergence difficulties.

The results of Figure 11 evaluate rollers made from all three materials. As stated previously, the models assume purely elastic deformation. In reality, elastomers will exhibit some hysteresis (See Diehl, 1995b,c). For rolling problems (cyclic deformations), material hysteresis will influence the results. Figures 11c and d depict how the influence of material hysteresis was removed (via an approximate method) from the experimental data. Comparing Figures 11e - g demonstrates that the models capture the dominate behavior and provide sufficient accuracy for use in nip-system design.

Figure 12 summarizes a study of sheet skew. A large 3-D ABAQUS/Explicit model is utilized. For computational efficiency, a non-traditional mesh (Figure 12b) is used to represent the tire. The model uses Explicit's contact surface capability to apply the appropriate constraints to make sure the mesh is valid. The results of Figure 12e demonstrate that the purely elastic model produces acceptable predictions compared to the actual test data.[1]

5.0 Conclusions

Analyzing media transport can effectively be performed with ABAQUS. Comparisons with several experimental results and published solutions have demonstrated the accuracy and usefulness of ABAQUS for this class of problems. This research has demonstrated how to use various capabilities of both Standard and Explicit to study quasi-static and dynamic issues. Application of this research has significantly improved our understanding of media transport and our ability to predict it.

Acknowledgments

The author's general work in this field has been strongly influenced by many members of the Mechanics of Flexible Structures Project at Penn State, especially Richard C. Benson and Kenneth D. Stack (formally at the University of Rochester). Special thanks are owed to Joop Nagtegaal and the HKS development and support staff for their valued advice and generous assistance. The author would like to thank Eastman Kodak Company for all their financial support, especially Woody Noxon, Bill Hunt, and Steve French. The valued technical discussions of Kodak engineers Gary Bisson, Eric Shih, and Tim Young are acknowledged.

References

Benson, R. C., "The Deformation of a Thin, Incomplete, Elastic Ring in a Frictional Channel," *Journal of Applied Mechanics,* Vol. 48, No. 4, Dec. 1981, pp. 895-891.

Benson, R. C., "The Feeding of a Thin, Inextensible Beam onto a Rigid Surface," *MFSP Internal Report*, Department of Mechanical Engineering, University of Rochester, NY, 1983.

Blatz, P. J., Ko, W. L., "Application of Finite Elastic Theory to the Deformation of Rubbery Materials," *Transactions of the Society of Rheology*, VI, 1962, pp. 223-251.

1. Because of the complexity in this particular problem, it was not possible to remove the influence of material hysteresis from the experimental data.

Brockman, R. A., "On the Use of the Blatz-Ko Constitutive Model in Nonlinear Finite Element Analysis," *Computers & Structures,* Vol. 24, No. 4, 1986, pp. 607-611.

Burden, R. L., Faires, J. D., *Numerical Analysis*, Third Edition, Prindle, Weber & Schmidt, Boston, 1985.

Diehl, T., "Formulation of a User MPC to Simulate Beam-Type Transport Problems," *MFSP Internal Report,* Department of Mechanical Engineering, University of Rochester, NY, June, 1993.

Diehl, T., "Simulating the Transport of Very Flexible Sheets," *ABAQUS User's Conference Proceedings,* Aachen, Germany, June, 1993.

Diehl, T., "Methods of Improving ABAQUS/Standard Predictions for Problems Involving Sliding Contact," *ABAQUS User's Conference Proceedings,* Paris, France, June, 1995.

Diehl, T., "Two-Dimensional and Three-Dimensional Analysis of Nonlinear Nip Mechanics with Hyperelastic Material Formulations," *Ph. D. Thesis,* University of Rochester, NY, 1995.

Diehl, T., "Modeling Foamed Elastomeric Tires with Ogden-Hill Strain-Energy Functions," *Proceedings of the Symposium on Numerical Implementation and Application of Constitutive Models in the Finite Element Method,* International Mechanical Engineering Congress, San Francisco, CA, November, 1995.

Johnson, K. L., *Contact Mechanics*, Cambridge University Press, Cambridge, 1989.

Soong, T. C., Li, C., "On the Unbonded Contact Between Plates and Layered Cylinders," *Journal of Applied Mechanics*, Vol. 47, December, 1980, pp. 841-846.

Soong, T. C., Li, C., "The Steady Rolling Contact of Two Elastic Layer Bonded Cylinders With a Sheet in the Nip," *International Journal of Mechanical Science*, Vol. 23, 1981, pp. 263-273.

Soong, T. C., Li, C., "The Rolling Contact of Two Elastic-Layered-Covered Cylinders Driving a Loaded Sheet in the Nip," *Journal of Applied Mechanics*, Vol. 48, December, 1981, pp. 889-894.

Stack, K. D., Benson, R. C., Diehl, T., "On the Inverse Elastica Problem and Its Application to Paper Handling," *Proceedings of the Symposium on Inverse Problems in Computational Mechanics*, International Mechanical Engineering Congress, Chicago IL, November, 1994.

Stack, K. D., "A Nonlinear Finite Element Model of Axial Variation in Nip Mechanics With Applications to Conical Rollers," *Ph. D. Thesis,* University of Rochester, 1995.

Stolte, J., "An Extending Dynamic Elastica: Analysis of Deformation Due To Inertial Loads and Impact With a Surface," Ph.D. Dissertation, Department of Mechanical Engineering, University of Rochester, NY, 1992.

Timoshenko, S. P., Gere, J. M., *The Theory of Elastic Stability*, McGraw-Hill, New York, 1961.

a) Transporting media through a nip

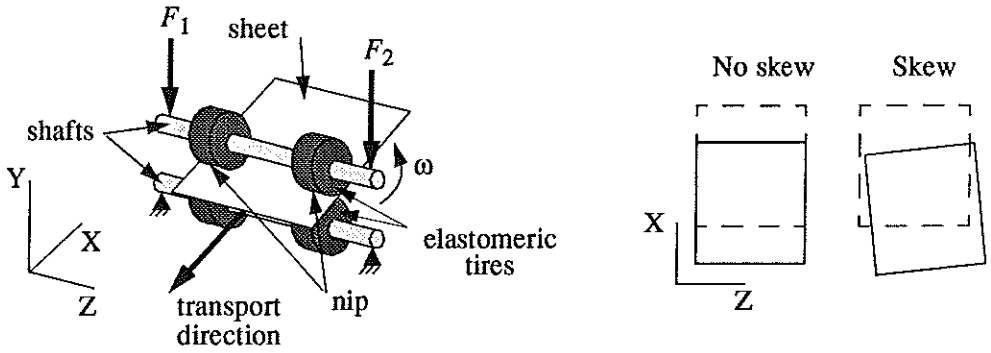

b) Transporting media in a channel: evaluating jams

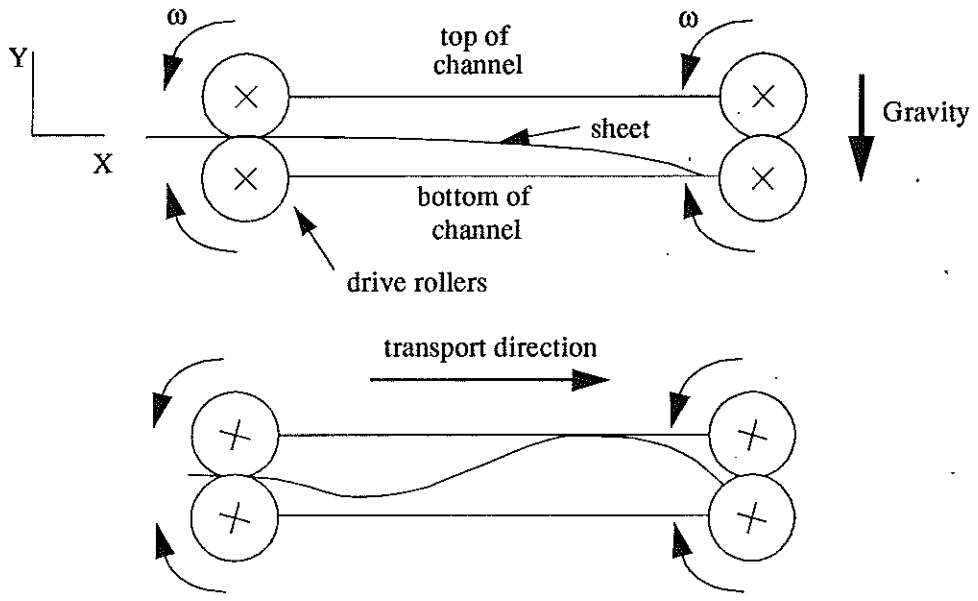

Figure 1: Schematics of media transport problems.

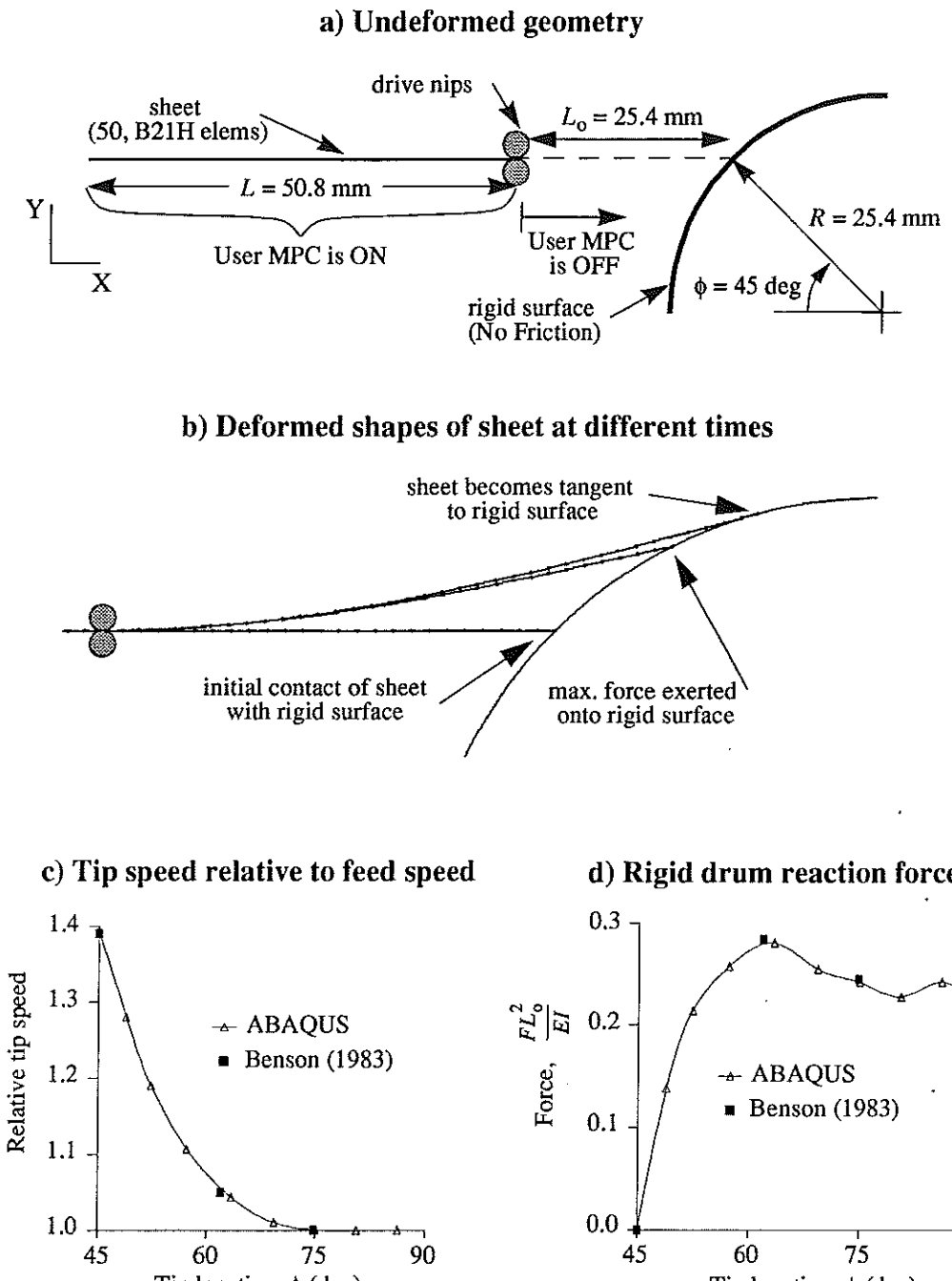

Figure 2: Quasi-static feeding of a sheet onto a frictionless circular drum. Gravity loading is not included.

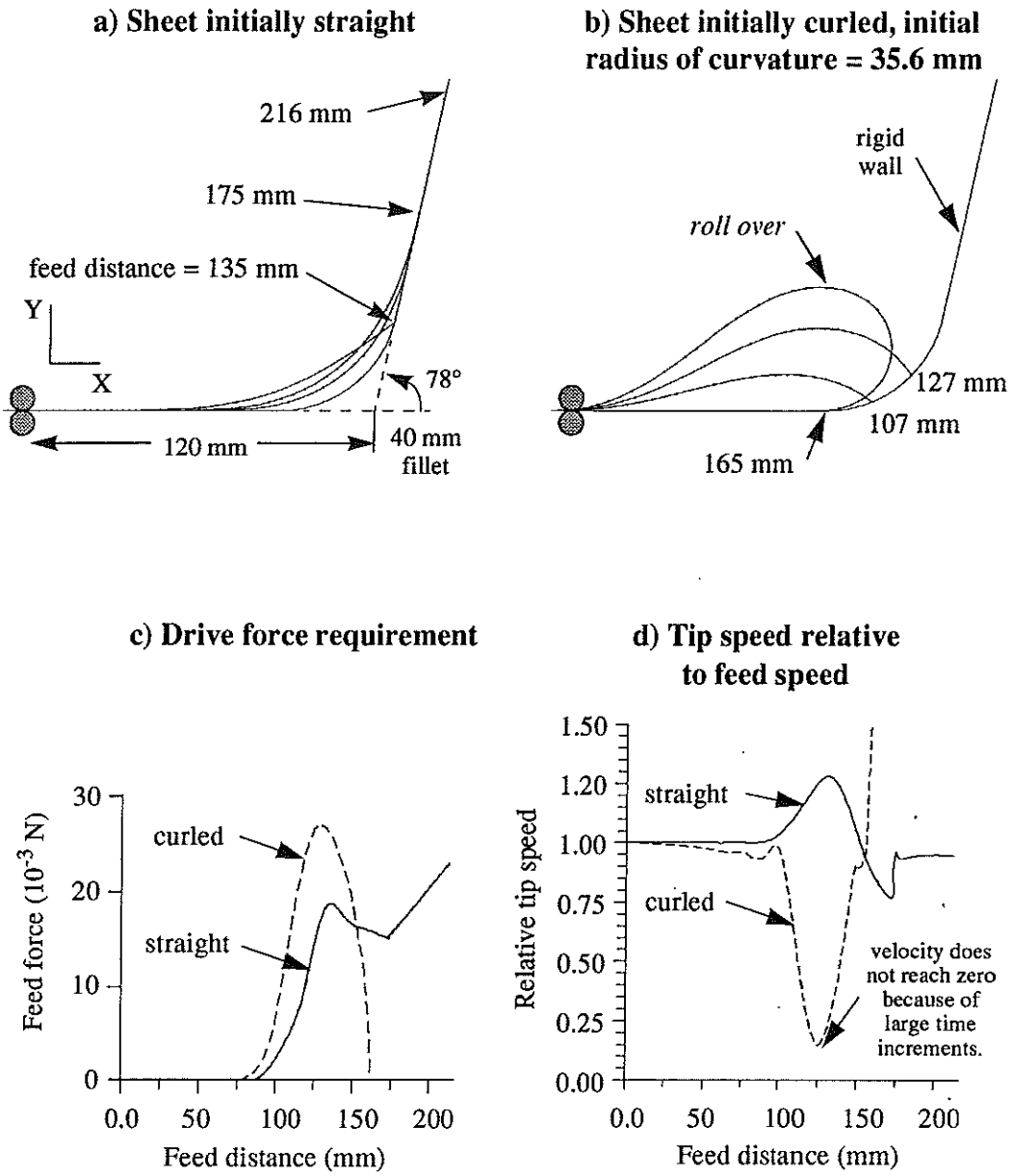

Figure 3: Feeding straight and curled media onto a curved rigid wall. Gravity loading is included.

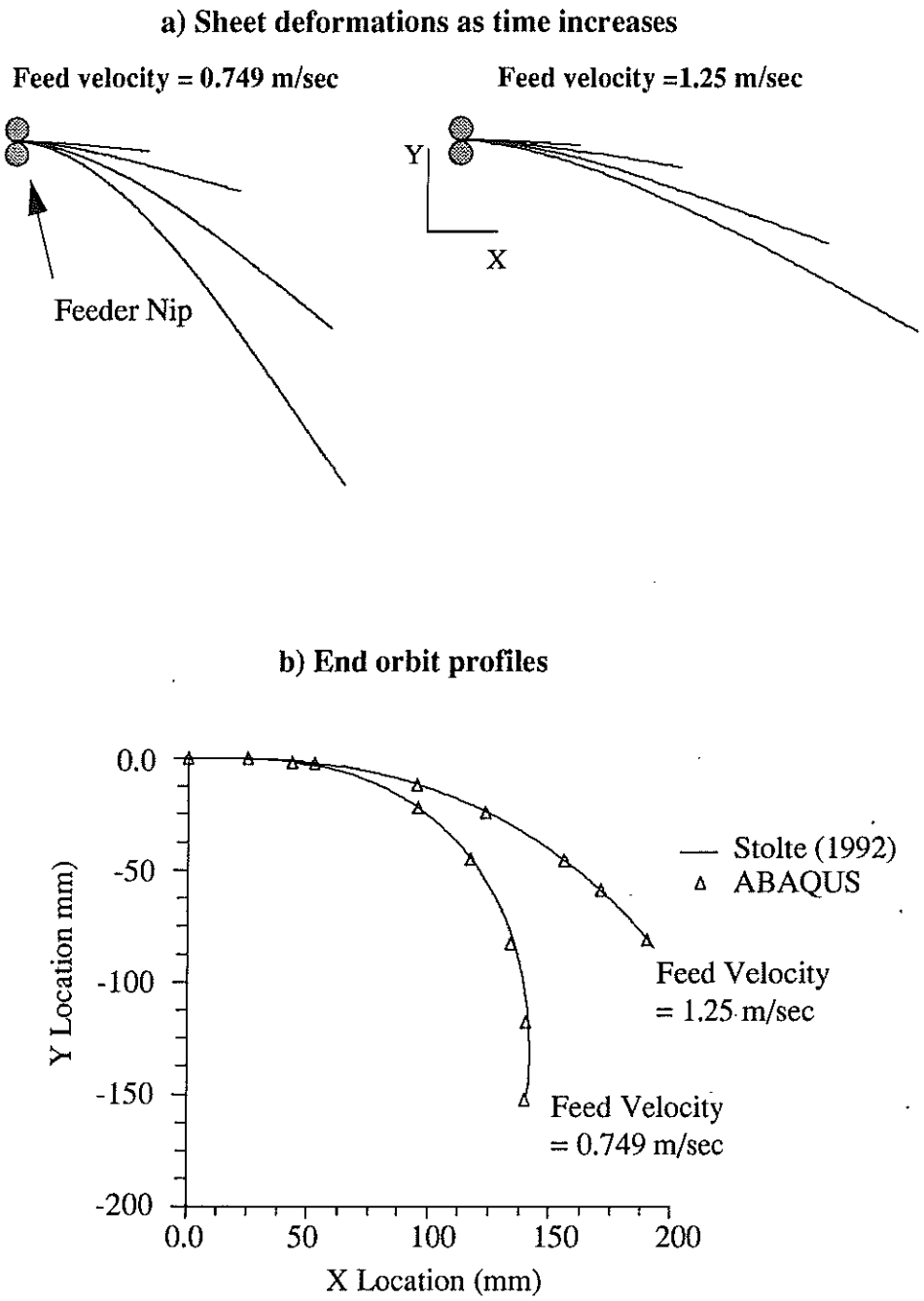

Figure 4: Dynamic extension of a sheet into a gravity field at different feed velocities.

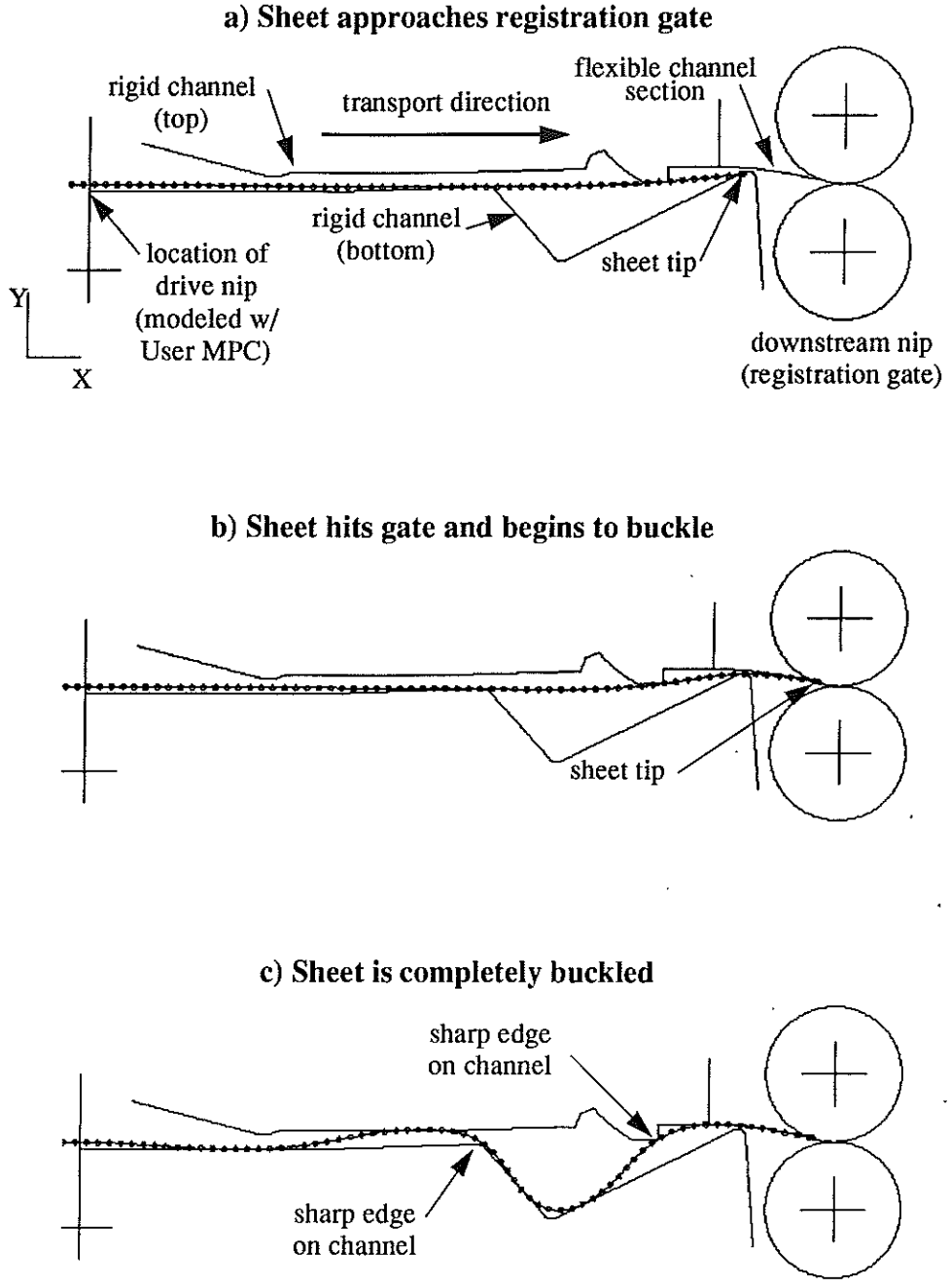

Figure 5: Transport analysis for registration problem.

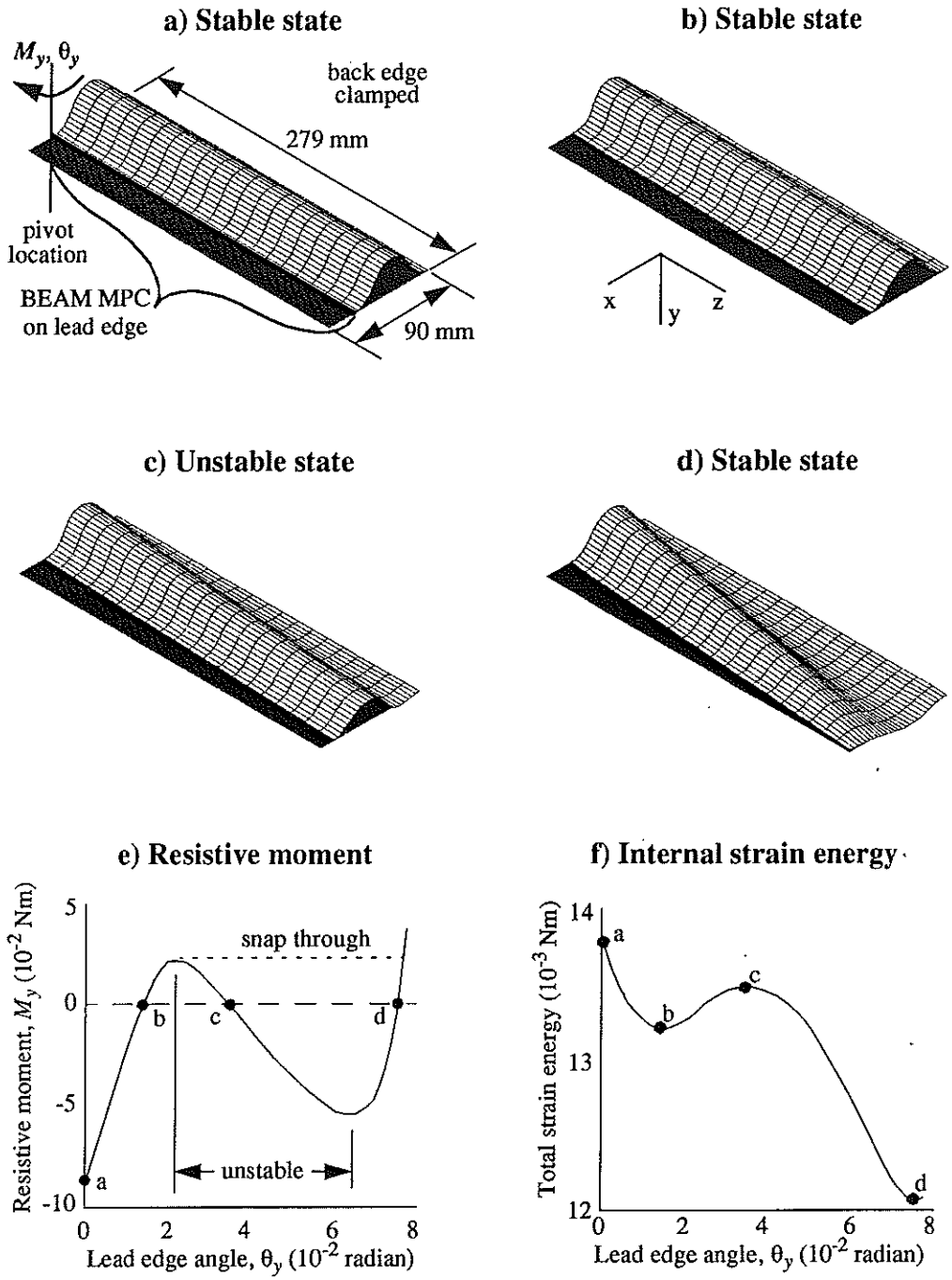

Figure 6: Alignment analysis for registration problem. Solution shown for a buckle height of 27mm.

a) Uniaxial compression

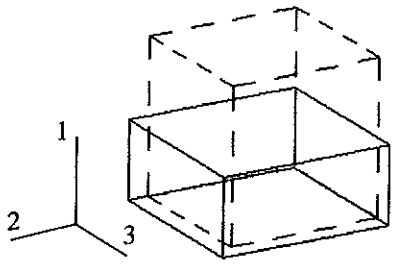

$$\lambda_1 = \lambda_{applied}$$
$$\sigma_2 = \sigma_3 = 0$$

b) Simple shear

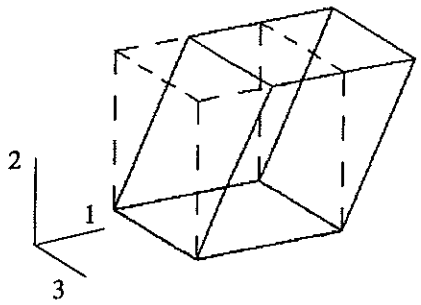

$$\mathbf{F} = \begin{bmatrix} 1 & \gamma & 0 \\ 0 & 1 & 0 \\ 0 & 0 & 1 \end{bmatrix}$$

c) Schematic of simple-shear testing apparatus

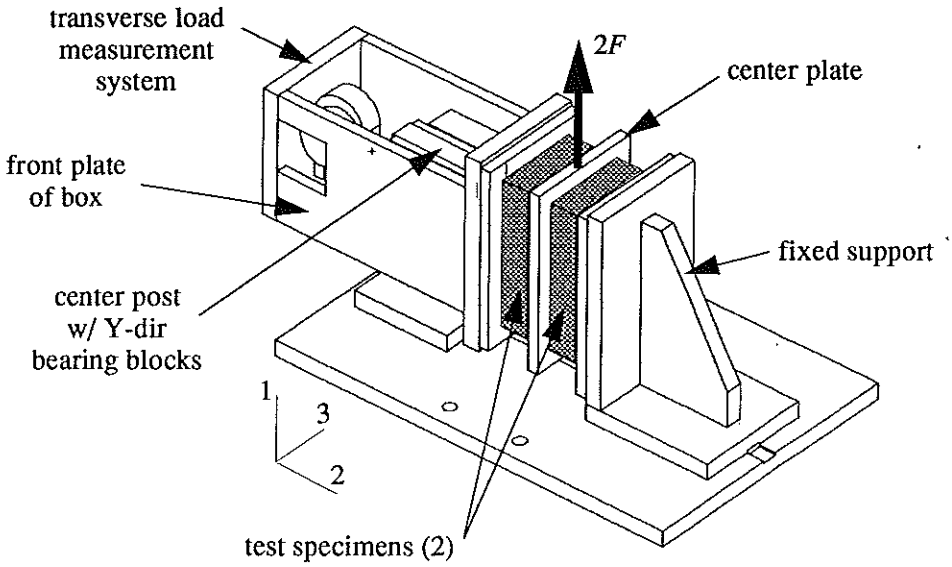

Figure 7: Deformation modes used for material testing of foamed elastomers.

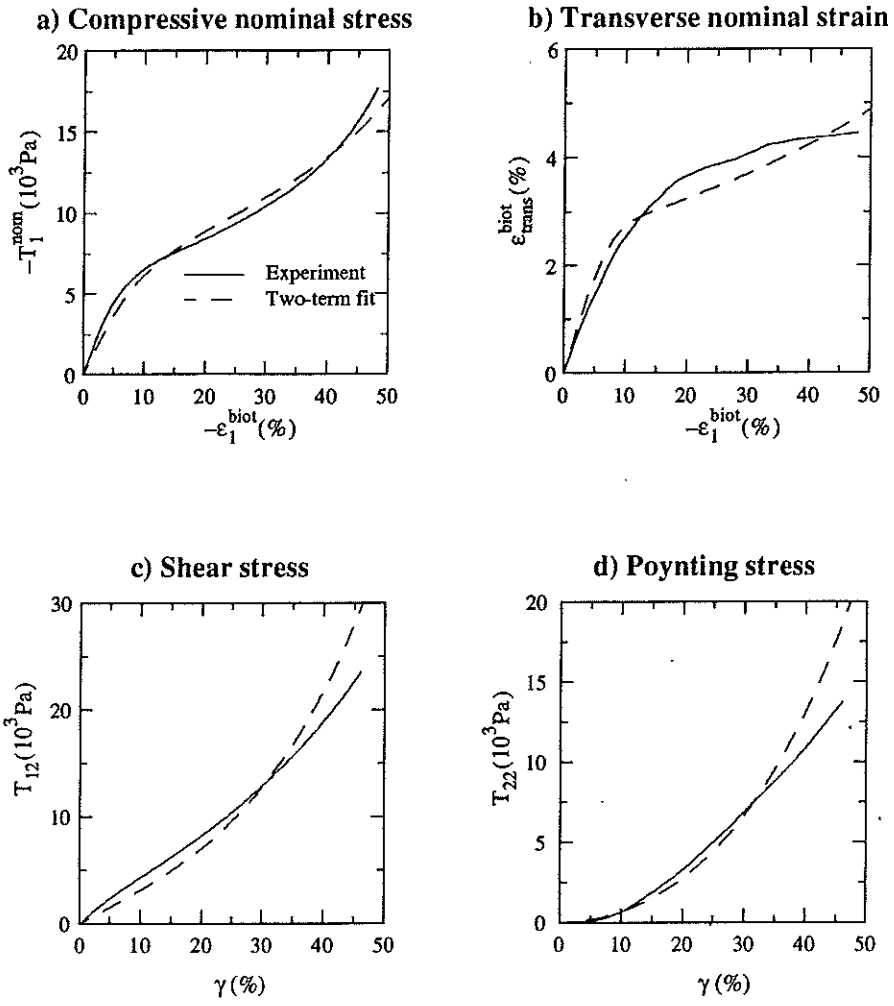

N	μ_1 (10^3 Pa)	μ_2 (10^3 Pa)	$\mu_0 = \mu_1 + \mu_2$ (10^3 Pa)	α_1	α_2	ν_1	ν_2
2	32.6	-2.97	29.6	10.05	3.293	0.039	0.514

Figure 8: Two-term Ogden-Hill fit to R600U data.

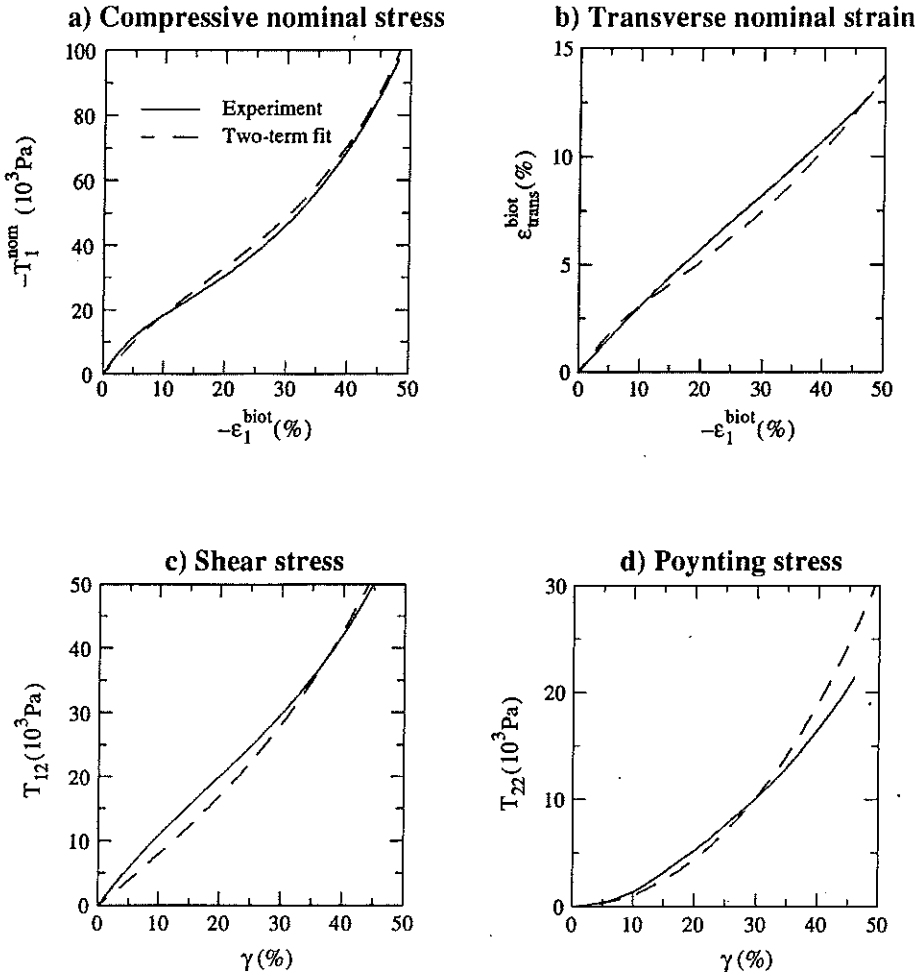

N	μ_1 (10^3 Pa)	μ_2 (10^3 Pa)	$\mu_0 = \mu_1 + \mu_2$ (10^3 Pa)	α_1	α_2	ν_1	ν_2
2	82.4	-3.87	78.5	7.22	2.34	0.176	0.508

Figure 9: Two-term Ogden-Hill fit to SE410 data.

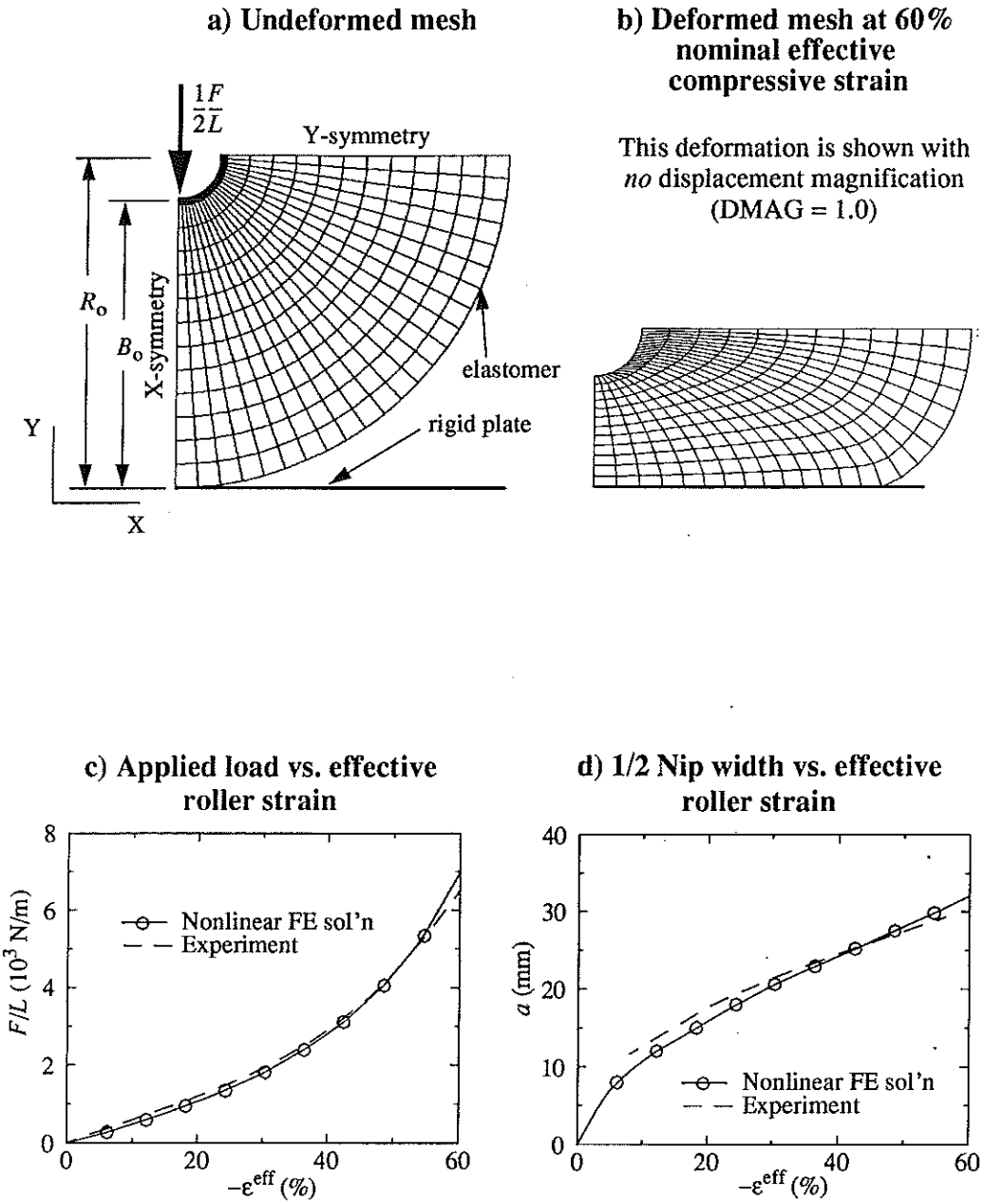

Figure 10: Finite element prediction compared to experimental data: nonrolling SE410 tire compression test.

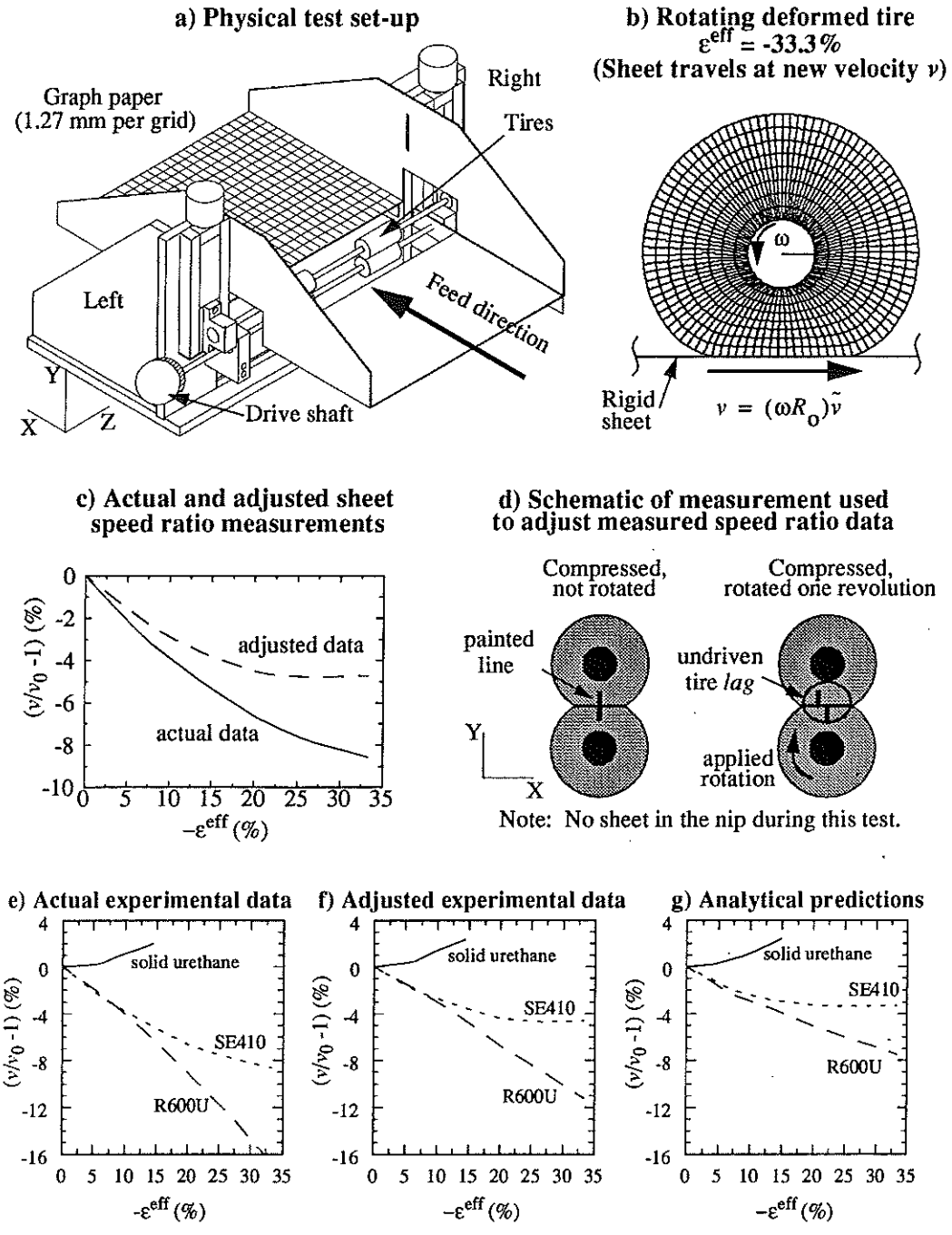

Analytical predictions are based on plane strain models for SE410 and R600U and a 3-D model for solid urethane.

Figure 11: Comparison of experimental data and Explicit finite element models: transport of a stiff sheet.

a) Complete 3-D model of system

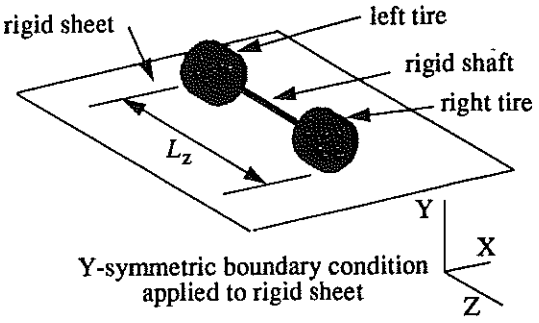

b) Close-up of 3-D model of tire

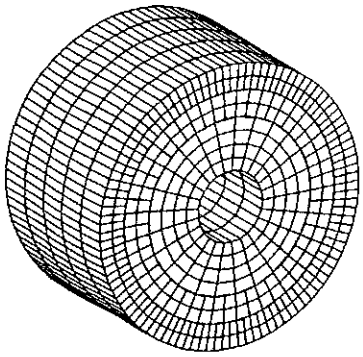

c) Definition of sheet skew

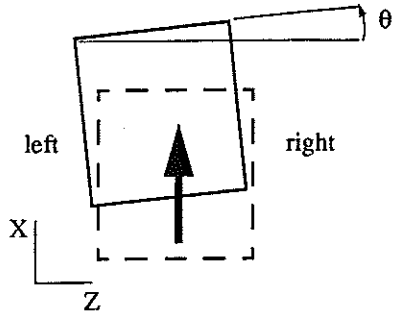

d) Effective roller strains applied

ε_{left}^{eff} (%)	$\varepsilon_{right}^{eff}$ (%)	$\Delta\varepsilon^{eff} = \varepsilon_{right}^{eff} - \varepsilon_{left}^{eff}$ (%)
-9.6	-13.8	-4.2
-12.3	-14.4	-2.1
-15.0	-15.0	0.0
-17.7	-15.6	2.1
-20.4	-16.2	4.2

e) Sheet skew experimental data and analytical predictions

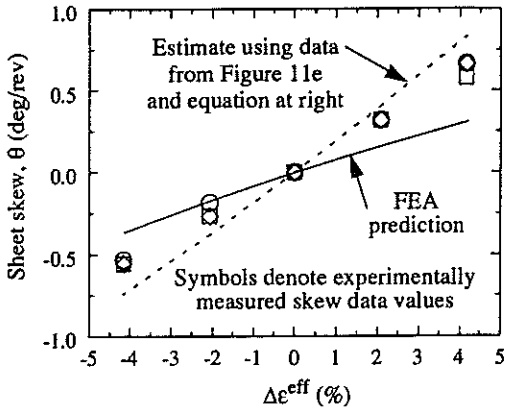

Estimate of skew:

$$\theta \approx \frac{R_o(\tilde{v}_{right} - \tilde{v}_{left})}{L_z}$$

Figure 12: Results from R600U nip system sheet skew evaluation.